ORIGINAL

Prediction of wood stiffness, strength, and shrinkage in juvenile wood of radiata pine

**Miloš Ivković · Washington J. Gapare ·
Aljoy Abarquez · Jugo Ilic · Michael B. Powell ·
Harry X. Wu**

Abstract Development of optimal ways to predict juvenile wood stiffness, strength, and stability using wood properties that can be measured with relative ease and low cost is a priority for tree breeding and silviculture. Wood static modulus of elasticity (MOE), modulus of rupture (MOR), radial, tangential, and longitudinal shrinkage (RS, TS, LS), wood density (DEN), sound wave velocity (SWV), spiral grain (SLG), and microfibril angle (MFA) were measured on juvenile wood samples from lower stem sections in two radiata pine test plantations. Variation between inner (rings 1–2 from pith) and outer (rings 3–6 from pith) rings was generally larger than that among trees. MOE and MOR were lower (50%) in inner-rings than in outer-rings. RS and TS were higher (30–50%) for outer-rings than inner-rings, but LS decreased rapidly (>200%) from inner-rings to outer-rings. DEN had a higher correlation with MOR than with MOE, while MFA had a higher correlation with dry wood MOE than with MOR. SLG had higher significant correlation with MOE than with MOR. DEN and MOE had a weak, significant linear relationship with RS and TS, while MOE had a strong negative non-linear relationship with LS. Multiple regressions had a good potential as a method for predicting billet stiffness ($R^2 > 0.42$), but had only a weak potential to predict wood strength and shrinkage ($R^2 < 0.22$). For wood stiffness acoustic velocity measurements seemed to be the most practical, and for wood strength and stability acoustic velocity plus core

M. Ivković (✉) · W. J. Gapare · A. Abarquez · H. X. Wu
CSIRO Plant Industry, P.O. Box E4008, Canberra, ACT 2604, Australia
e-mail: Milosh.Ivkovich@csiro.au

J. Ilic
Forest and Wood Products Australia, P.O. Box 69, World Trade Centre, Melbourne,
VIC 8005, Australia

M. B. Powell
Southern Tree Breeding Association Inc, P.O. Box 1811, Mt. Gambier,
SA 5290, Australia

density seemed to be the most practical measurements for predicting lower stem average in young trees.

Introduction

In Australia, structural timber is machine-stress-graded using the Australian and New Zealand standard AS/NZS 4063 (1992). Wood stiffness, measured as modulus of elasticity (MOE), is one of the most important mechanical properties for structural end-uses and has a direct impact on structural timber grade outturn. Wood strength of stress-graded timber is measured as modulus of rupture (MOR). Standard requirements for wood stiffness and strength are given in AS/NZS 1748 (1997). Dimensional stability is also important for structural timber performance, and in this study, three measures of wood shrinkage were used (tangential, radial, and longitudinal shrinkage, denoted as TS, RS, and LS, respectively).

In radiata pine (*Pinus radiata*), the juvenile wood comprises anywhere from the first seven to the first 13 rings from the pith, and often presents issues for utilisation due to its poor mechanical properties and high distortion (Zobel and Sprague 1998; Burdon et al. 2004; Gapare et al. 2006, 2007). As radiata pine crop rotation becomes shorter due to genetic improvement and modern silvicultural regimes, the proportion of juvenile wood will be higher. Besides lower wood stiffness and strength, dimensional instability (shrinkage) is also a problem in juvenile wood, in which microfibril angle (MFA) ($>20°$) and spiral grain (SLG) ($>5°$) are larger and coupled with a significant amount of compression wood. Defects such as twist, bow, and crook often occur in sawn products made from trees with a high proportion of juvenile wood harvested in fast grown plantations (Zobel and Sprague 1998). Differential wood shrinkage within a piece of timber causes such timber deformations. Twist is the main form of instability of radiata pine timber (Cown et al. 1996a) and can be explained by variation in SLG and LS and TS (Johansson and Bäkström 2002). Bow and crook in timber can be explained mainly by differential LS (Johansson 2003). Consequently, one of the main impediments for greater market acceptance of fast grown radiata pine wood is the low stiffness, strength, and poor dimensional stability of its juvenile core (Cown and van Wyk 2004).

Methods to predict juvenile wood stiffness, strength, and stability using wood traits that can be measured with relative ease and low cost are essential for breeding programs to rank selections. To predict juvenile wood stiffness, strength, and stability of radiata pine trees, consideration must be given to within-tree variation of these traits. Wood stiffness in radiata pine increases radially from pith to bark, but the greatest changes occur near the pith (Xu and Walker 2004). Maps of wood properties including MOE have been created using SilviScan™ data in radiata pine (McKinley et al. 2003). Variation in shrinkage has also been shown to be a predictable pattern within a tree. Transverse (radial and tangential) shrinkage values are lower in the corewood zone (near the pith), but LS values are higher (Cown et al. 1991; Harris 1997; Gapare et al. 2008).

An understanding of the relationship between the mechanical performance of wood and physical and anatomical properties such as wood density (DEN), cell wall thickness, MFA and SLG would also assist the prediction of wood quality based on basic traits. DEN is a measure of the relative amount of cell wall material, and therefore an important trait for predicting strength properties (Pashin and de Zeeuw 1980). However, microfibril orientation in the S2 layer of cell walls is considered to be the most important factor determining wood stiffness, in the juvenile wood zone (Xu and Walker 2004). The negative influence of SLG on mechanical properties of clear wood samples is also significant (Cave 1969; Cown et al. 1996b; Tsehaye and Walker 1996; Cown 1999).

The causes of shrinkage can be examined at molecular, ultrastructural, microscopic, and macroscopic levels (Astley et al. 1997). At the molecular level, cellulose and hemicelluloses are responsible for adsorption and desorption of water molecules, while lignin and extractives are retarding water penetration into cellulose. At the higher levels of wood structure, shrinkage of wood cells is considered to be dominated by tracheid wall thickness, lumen shape, effects of rays and bordered pits, and by the disposition of MFAs. In multi layers of wood with variable shrinkage properties (e.g. earlywood and latewood, or juvenile and mature wood), stresses develop from restraints between layers (Barber and Meylan 1964; Cave 1972; Pang 2002). Based on wood structure, slope of grain does not cause LS directly, but a component of TS tends to act in a longitudinal direction (Haslett et al. 1992). In juvenile wood of fast grown trees often with wide rings, ring curvature may have a similar effect as SLG (Pashin and de Zeeuw 1980).

Although statistical methods cannot explain the exact behaviour of any particular wood cut, they can predict the average trends. Partial regressions and path analyses have been used to untangle the relationships between wood traits affecting stiffness and strength, and shrinkage. DEN and MFA have strong correlations with the stiffness and strength of clear wood (e.g. Ying et al. 1994; Matheson et al. 1997; Downes et al. 2002). Several authors reported a non-linear relationship between LS and MFA in pines (Harris and Meylan 1965; Meylan 1967; Megraw et al. 1999). Other authors found that both SLG and MFA would be good predictors of LS (Evans and Ilic 2001). Indirect prediction of stiffness and/or shrinkage is possible using the component traits determined by sophisticated instruments such as SilviScan[TM] (Evans 2003). More recently, measurements of sound velocity are probably the most practical predictors of wood quality, with potential utility for identifying not only low stiffness but also distortion-prone wood (Ilic 2004).

Direct assessment of stiffness, strength, and stability is time consuming, expensive, and destructive. Development of optimal ways to predict clear wood stiffness, strength, and stability using non-destructive measurements would be of great importance to tree breeders, silviculturists, and wood processors. The specific objectives of this study were to:

1. examine pith-to-bark variability of wood stiffness and strength, and TS, RS, and LS of 7–8 year-old radiata pine;
2. examine causal relationships between stiffness, strength, shrinkage, and basic wood properties; and

3. develop optimal ways for prediction of clear wood stiffness, strength and stability by non-destructive measurement of wood properties.

Materials and methods

The study was based on two genetic trials located in Victoria at Flynn and in South Australia at Kromelite and the details of site characteristics are provided in Table 1.

At Flynn site, there were 250 genotypes (full- and half-sib families) planted in four-tree row-plots within five complete replication blocks. One randomly chosen tree from each genotype in each of two replications was felled, and a stem section (billet) about 70 cm in length was sampled between 0.5 and 2.0 m from ground. The billet was cut into three sub-samples for shrinkage, SLG and stiffness measurements according to Fig. 1. Kromelite site had 110 genotypes represented by four-tree row-plots in five replication blocks. One tree from each genotype in each of three replications was sampled. Sampled trees in each trial had previously been cored and had stem sound velocity measured by IML hammer (http://www.walesch.ch). The measurements on standing trees, increment cores and billets were carried out as follows.

Wood density, microfibril angle and stiffness measurements on increment cores using SilviScan

Twelve millimetre bark-to-bark increment cores were collected at breast height (1.3 m) from 980 trees at Flynn and 660 trees at Kromelite in 2003, before the billets were sampled in 2004. Whole core basic density (DEN_{ic}) was assessed gravimetrically, as dry weight over green volume. Bark-to pith cores from 830 trees felled in 2004 were also assessed by SilviScan[TM] (Evans et al. 1996). Density (DEN_{ss}) at 12% moisture content was measured at 50 μm intervals, while MFA_{ss} was measured over 5 mm intervals. SilviScan measurements were used to obtain individual ring values MOE_{ss}, and ring-area weighted averages. Ring-area weighted data from cores were matched with the corresponding rings present in the shrinkage and static measurement sample blocks.

Table 1 Characteristics of the Flynn and Kromelite sites used for this study

Site	Flynn	Kromelite
Date planted	6/1996	7/1997
Cambial age at time of sampling	8	7
Spacing	3.6×2.5 m	2.74×2.5 m
Latitude	38°14′S	37°50′S
Longitude	146°45′E	140° 55'E
Elevation (m)	166	55
Annual rainfall (mm)	760	900
Soil type	Sandy loam	Sandy clay-loam
Site type	Second rotation	Second rotation

Cut face

Pith

Shrinkage
sample (x3)
B, C, D

20mm

20mm

150mm

B

C

D

Cut face

Compression
Wood
Image

Spiral grain
sample
A

12mm Core
sample hole

A

12mm

Pith

Cut face

Clearwood samples
for MOE (x3)
E, F, G

Paddle pop stick
with 2 seasons of
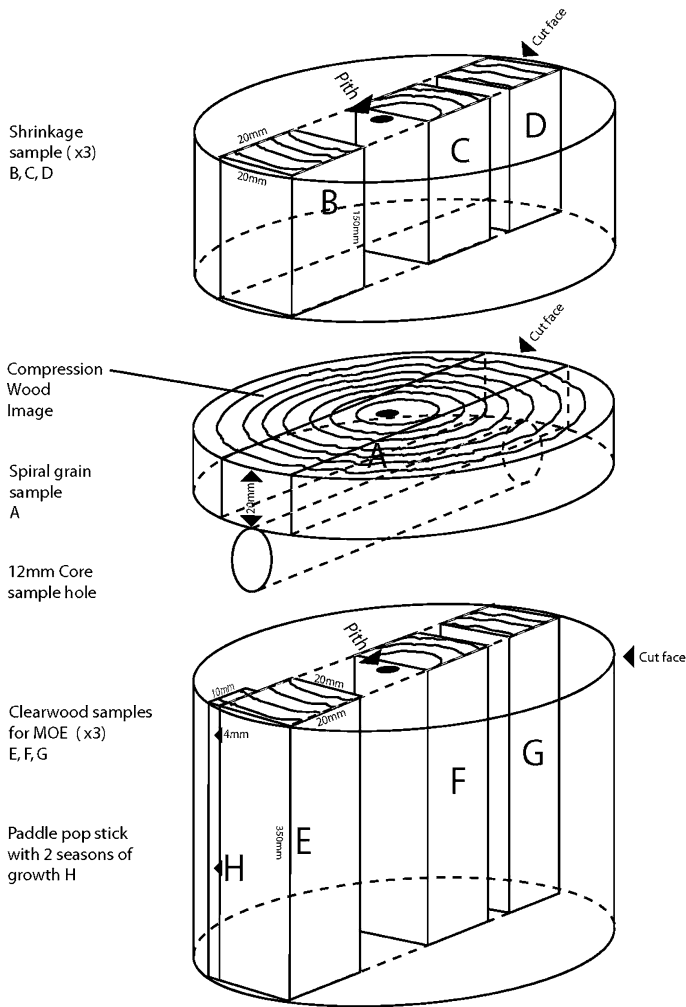growth H

10mm

20mm

20mm

4mm

350mm

H

E

F

G

Fig. 1 Sub-sampling of billets (stem sections) harvested from Flynn and Kromelite sites

Standing tree stiffness measurement using sound velocity

An IML hammer (stress wave timer) was used to measure the sound wave time-of-flight in standing trees that were previously cored. The standing tree time-of-flight technique was used on one side of the stem. This involved inserting two probes 1 m apart along the axis of the tree. The bottom probe was tapped with the IML hammer which has one transducer. The second transducer detects the stress wave upon arrival, and the electronics determine the time of flight.

The acoustic SWV is related to MOE_{iml} of the wood according to the following equation:

$$SWV^2 = MOE/DEN$$

and

$$SWV = 1/T$$

where SWV is sound wave velocity (m s^{-1}); T is time of flight (m s^{-1}); MOE is modulus of elasticity (GPa) and DEN is bulk density (kg/m^3), usually assumed to be 1,000 kg/m^3 for radiata pine. When MOE is measured in this way it is known as dynamic MOE$_{iml}$ in contrast to static MOE which is measured by bending. The dynamic and static stiffness values are highly related in green and dry wood (Booker and Sorensson 1999; Ilic 2001a).

Spiral grain measurement

A total of 466 and 308 trees from Flynn and Kromelite, respectively, were used for the testing. Stem discs were air dried at $25 \pm 5°C$ for 6 months. Each disc sample was sawn into a 3.5×5 cm^2 diametrical strip following a North–South axis through the stem, including at least part of the pith. Along the length of each flitch, a flat surface was created using a belt sander to provide a plane of reference for SLG measurement. Growth rings were numbered according to their calendar year of formation, counting inwards from the cambium. A chisel and mallet were used to split the samples on the outermost boundary of each annual latewood band. SLG angle was measured using a pivoting digital protractor attached to a fixed platform. Mean grain angle for each ring was obtained by adding the measurements on two opposing radii and dividing by two. The mean grain angle in each ring can be considered a measure of average grain angle deviation from the vertical axis of the cambial cylinder in each year of growth (e.g. Hansen and Roulund 1998; Gapare et al. 2007).

Shrinkage and dynamic stiffness measurement on shrinkage samples

The procedures for determining shrinkage were similar to those used by Kingston and Risdon (1961). The three samples (B, C, and D) cut from the shrinkage billet (see Fig. 1) were measured initially in a green state and subsequently oven dried at $103 \pm 2°C$ to determine shrinkage. Moisture content based on oven-dry weight was determined before and after reconditioning. For each of the three samples, radial, tangential, and longitudinal dimensions were measured using a digital displacement gauge with readings graduated to 0.001 mm. The shrinkage value for RS, TS, and LS were expressed as a percentage (%) of the green measurement. Anisotropic shrinkage ratio was calculated as TS/RS. Average values for samples B and D represented the outer rings (rings 4–6 at Flynn; and rings 3–5 at Kromelite) whereas C represented the inner rings (rings 1 and 2) close to the pith. Radial gradient (pith to bark) can be defined as the difference in shrinkage between outer and inner rings.

Due to ring angle caused by the wandering pith in sample C and to some extent ring curvature close to the pith it is generally not possible to get valid TS and RS values for the inner-rings closest to the pith. This is partly because shrinkage close

to the pith will be a function of both RS and TS. Adjustments for ring curvature were made following the method of Dumail and Castera (1997), but this had small overall effects. SLG contributes to LS, so none of the shrinkage measurements had strictly "true direction". In addition, samples from juvenile core were distorted upon drying. This presented a problem in accurately measuring the length of samples as the curvature present exaggerated the extent of measured shrinkage. The maximum point of sample curvature was measured and a correction factor to the final length measurement was incorporated. On small clear (shrinkage) samples B, C, and D, dynamic MOE_{sc} was also measured using the acoustic resonance method developed by CSIRO (Ilic 2001a).

Dynamic and static stiffness and strength measurement on clear wood samples

Three samples (E, F, and G) with 20×20 mm in cross section and 350 mm in length were cut from the stiffness billet (see Fig. 1, bottom). Dynamic and static MOE_{sc} and MOR_{sc} was measured on each of the three samples. Dynamic MOE_{sc} was also measured using the CSIRO acoustic resonance method (Ilic 2001a). Static bending tests were carried out using three-point bending test on Instron machine, according to the standard procedure (Mack 1979).

Dynamic stiffness measurement using small axial sample ("paddle-pop")

A small ($350 \times 10 \times 4$ mm) clear sample (H) was cut radially along the bottom billet near the bark (Fig. 1). The purpose of this sample was to assess predictability of the log stiffness based on a surface sample ("paddle-pop") dynamic MOE_{pp}, as first proposed by Ilic (2001b, 2003). The samples were oven-dried and re-equilibrated to room conditions.

Statistical analyses

Average stiffness, strength, and shrinkage

Before embarking on analyses, area-weighted billet average for stiffness, strength, and shrinkage was calculated. The billet averages were used as a benchmark value that was wanted to predict based on non-destructive samples.

Average billet values of stiffness were calculated from measurements on samples B, C, and D (acoustic) and E, F, and G (both static and acoustic). Three average values of stiffness were computed for inner-rings (ring 1–2 from pith), outer-rings (ring 3–6 from the pith) and whole billet. For inner-rings, the average (MOE_{in}) was obtained by averaging values for samples C and F. The outer-ring stiffness (MOE_{out}) was obtained by averaging values for samples B, D, E, and G. The whole billet value (MOE_{bil}) was obtained by area-weighting MOE_{in} and MOE_{out} using stem diameter based on core length. Basic DEN_{bil} was also obtained from samples B, C, D, E, F, and G by averaging in the same fashion.

Average values of strength for the billet were calculated from samples E, F, and G. For inner rings, MOR_{in} was the values taken from sample F. For outer rings, MOR_{out} was obtained by averaging values for samples E and G. Whole billet average strength (MOR_{bil}) was obtained by area-weighting MOR_{in} and MOR_{out}.

Average values of shrinkage (RS, TS, and LS) for the billet were calculated from samples B, C, and D. For inner rings, the values RS_{in}, TS_{in}, and LS_{in} were obtained from sample C. For outer rings, values RS_{out}, TS_{out}, and LS_{out} were obtained by averaging measurements for samples B and D. The whole billet averages (RS_{bil}, TS_{bil}, and LS_{bil}) were obtained by weighting values for inner and outer rings.

Variable transformations

Distributions of the measured traits were checked for normality using SAS interactive data analyses package (SAS Institute Inc. 2005). Most of the traits conformed to normality tests (KS statistic at $P > 0.01$ significance level) except for LS and the ratio of TS to RS (TS/RS). Log transformation was applied to LS in order to obtain an approximately normally distributed variable, and square-root arc-sine transformation was applied to TS/RS to normalize the proportion data.

Within-tree variation analysis

Pith-to-bark variation was analysed using inner-rings and outer-rings. Procedures ANOVA and VARCOMP in SAS 9.1 (SAS Institute Inc. 2005) were used to analyse variation from inner-rings to outer-rings and from two aspects (North and South).

Path analysis

Path analyses were used to examine casual models involving direct and indirect effects of independent variables and dependent response variables (e.g. Downes et al. 2002). Correlation analysis quantifies the linear relationship between two variables, but does not specify any cause/effect relationship. Path analysis partitions a correlation coefficient into a direct effect of the casual variable and indirect effects through alternate pathways to the response. Standardized partial regression coefficients are used to indicate strength and direction of direct effects (Li 1981). The standardized regression coefficient equals the value of the correlation coefficient between the variable of interest and the residuals from the regression, if the variable was omitted. The objective of our path analyses was to examine how much component wood quality traits such as ring width (RW), DEN, MFA, or SLG can explain wood stiffness, strength, and shrinkage.

Multiple regression analyses

To search for the optimal combination of component wood variables to predict wood stiffness, strength, and shrinkage, multiple regression analyses were used. The RW_{ss}, DEN_{ss}, MFA_{ss}, from increment cores, standing tree stiffness measurements from IML hammer (MOE_{iml}), and dynamic MOE_{pp} from "paddle-pop"

measurements were used as independent variables. The procedure PROC REG in SAS 9.1 (SAS Institute Inc. 2005) was used to fit multiple linear regression models. For each model, as an overall test of significance, multiple R^2 (average r^2 for the measured y's vs. the predicted y's) and root mean square error (RMSE) were used. For each independent variable, a regression coefficient (b) was obtained, with associated t and P values for conditional significance given all the other variables are in the model. Exploratory data analyses showed that dependent and independent variables were approximately normally distributed (KS statistic $P > 0.05$). Independent variables were also tested for co-linearity, and inter-correlations between independent variables would make estimation difficult (SAS Institute Inc. 2005). Residual plots were examined for patterns and outliers.

Results and discussion

Wood stiffness and strength

Within-tree variation and phenotypic correlation among wood traits

Wood stiffness in radiata pine increases radially from pith to bark, but the greatest change occurs in the wood near the pith (Downes et al. 2002; Xu and Walker 2004; Wu et al. 2005). Additionally, in the corewood zone, a rapid increase of wood stiffness occurs in the vertical direction (Xu et al. 2004). In general, wood stiffness follows distributions of basic wood traits such as cell wall thickness, DEN and MFA in both radial and axial directions (Megraw et al. 1998). In the current study, pith-to-bark variability of wood stiffness and strength was very high. Trait means for RW, DEN, SLG, MFA, MOE, and MOR based on inner-rings, outer-rings and weighted averages for the whole billet are presented in Table 2. There was an increase in DEN, stiffness, and strength from pith to bark. Variation in stiffness between inner-rings and outer-rings of the same tree was higher than variation between trees (MOE_{sc} VAR_{rings} = 5.6 vs. VAR_{trees} = 0.77). For MoE_{sc}, variation between North and South aspects accounted for 13.9%, sampling height (low vs. high samples, Fig. 1) accounted for 21.8% and variation among trees accounted for 64% of total variation. Such high within-tree variation renders sampling, measurement and prediction of whole billet averages using component wood traits highly challenging (Downes et al. 1997).

Correlations between inner and outer samples were all significant at $P < 0.0001$ and were $r = 0.56$ for DEN, $r = 0.61$ for MOE, and $r = 0.68$ for MOR. Generally, between-trait correlations were similar at Flynn and Kromelite for inner-rings, outer-rings or whole billet (Table 3). For whole billet, RW was not related to DEN and MOR, but showed a low but significant negative correlation with MOE, at both sites ($r > -0.15$). For inner-rings, RW had significant correlations with MOE ($r = -0.31$ at Flynn and $r = -0.21$ at Kromelite). Stiffness and strength measurements in the juvenile corewood were correlated with MFA and DEN, as previously found in pines (Cown et al. 1999; Megraw et al. 1998, 1999). However, in the whole billet samples, DEN had a higher correlation with MOR ($r = 0.62$ at Flynn and $r = 0.70$ at Kromelite) than with MOE ($r = 0.41$ at Flynn

Table 2 Sample means for inner-rings (rings 1–2) and outer-rings (rings 3–6) and weighted averages for the whole billet at Flynn (F) and Kromelite (K) sites

Trait	Site	RW_{ss}[a] (mm)	DEN_{sc}[b] (kg/m³)	SLG_{ds}[c] (deg)	MFA_{ss}[a] (deg)	MOE_{sc}[b] (GPa)	MOR_{sc}[d] (MPa)
Billet	F	12.5	388	4.0	28.5	5.8	50.7
	K	15.1	350	3.8	31.7	4.5	40.9
Inner-rings	F	17.6	346	4.9	37.0	3.2	33.6
	K	23.7	310	4.6	37.2	2.6	30.9
Outer-rings	F	9.6	403	2.7	22.1	6.7	56.5
	K	8.8	367	3.4	27.3	5.1	49.2

[a] RW_{ss} and MFA_{ss} are based only on SilviScan increment cores

[b] DEN_{sc} and MOE_{sc} based on six small clear samples (BCDEFG)

[c] SLG_{ds} based on shrinkage disk samples

[d] MOR based on three clear-wood samples (EFG)

and $r = 0.50$ at Kromelite). In contrast, MFA had a higher correlation with MOE ($r = -0.60$ at Flynn and $r = -0.50$ at Kromelite) than with MOR ($r = -0.32$ at Flynn and $r = -0.27$ at Kromelite). Similarly, SLG had a higher significant correlation with MOE ($r = -0.24$ at Flynn and $r = -0.15$ at Kromelite, than with MOR ($r = -0.16$ at Flynn and $r = -0.18$ at Kromelite).

Table 3 Correlations between six wood traits for inner-rings, outer-rings, and whole billet (above-diagonal for Flynn and below-diagonal for Kromelite; values for billet, outer-rings, and inner-rings listed from top to bottom; correlations in bold are significant at $P < 0.01$)

	MOE	MOR	RW	DEN	MFA	SLG	
MOE		**0.71** / **0.73** / **0.66**	**-0.15** / **-0.16** / **-0.31**	**0.41** / **0.39** / **0.50**	**-0.60** / **-0.63** / **-0.42**	**-0.24** / **-0.21** / -0.09	Flynn
MOR	**0.71** / **0.72** / **0.66**		-0.08 / -0.07 / **-0.18**	**0.62** / **0.61** / **0.58**	**-0.32** / **-0.35** / **-0.24**	**-0.16** / -0.12 / -0.06	
RW	-0.12 / **0.17** / **-0.21**	0.05 / 0.12 / -0.12		-0.00 / 0.03 / **-0.20**	**0.48** / **0.41** / **0.45**	**0.14** / 0.04 / -0.04	
DEN	**0.50** / **0.36** / **0.37**	**0.70** / **0.69** / **0.64**	0.01 / 0.00 / -0.04		-0.12 / -0.09 / -0.09	-0.04 / -0.02 / -0.03	
MFA	**-0.50** / **-0.57** / **-0.37**	**-0.27** / **-0.27** / -0.12	**0.19** / **0.25** / **0.24**	0.05 / 0.03 / 0.12		**0.27** / **0.21** / -0.07	
SLG	**-0.15** / **-0.22** / -0.06	**-0.18** / **-0.20** / -0.10	0.03 / 0.04 / **0.22**	0.04 / -0.09 / -0.01	0.06 / 0.13 / -0.05		Kromelite

Causation from path analyses

Six wood variables listed in Table 2 and presented in Fig. 2 (RW, DEN, SLG, MFA, MOE, and MOR) for whole billet estimates were standardised for path analyses. Path diagrams are presented in Fig. 3. RW had a positive direct effect (path coefficient) on MOE ($pc_{RW\_MOE} = 0.18$), but a negative indirect effect through path connecting RW, MFA, and MOE (Fig. 3a). The indirect effect of RW on MOE was a result of the significant positive correlation between RW and MFA (Table 3).

In previous studies, MFA and DEN were important determinants stiffness, but MFA had a stronger effect (Cave and Walker 1994; Downes et al. 2002). Similar results were found in the current study. For instance, the direct effect of DEN on MOE was positive and significant but less than the effect of MFA (e.g. Flynn billet $pc_{DEN\_MOE} = 0.41$ vs. $pc_{MFA\_MOE} = -0.54$). That relationship held overall at average and outer sampling strata, but for inner samples the DEN effect was equal or even higher then MFA (e.g. Flynn in $pc_{DE\_MOE} = 0.46$ vs. $pc_{MFA\_MOE} = -0.35$).
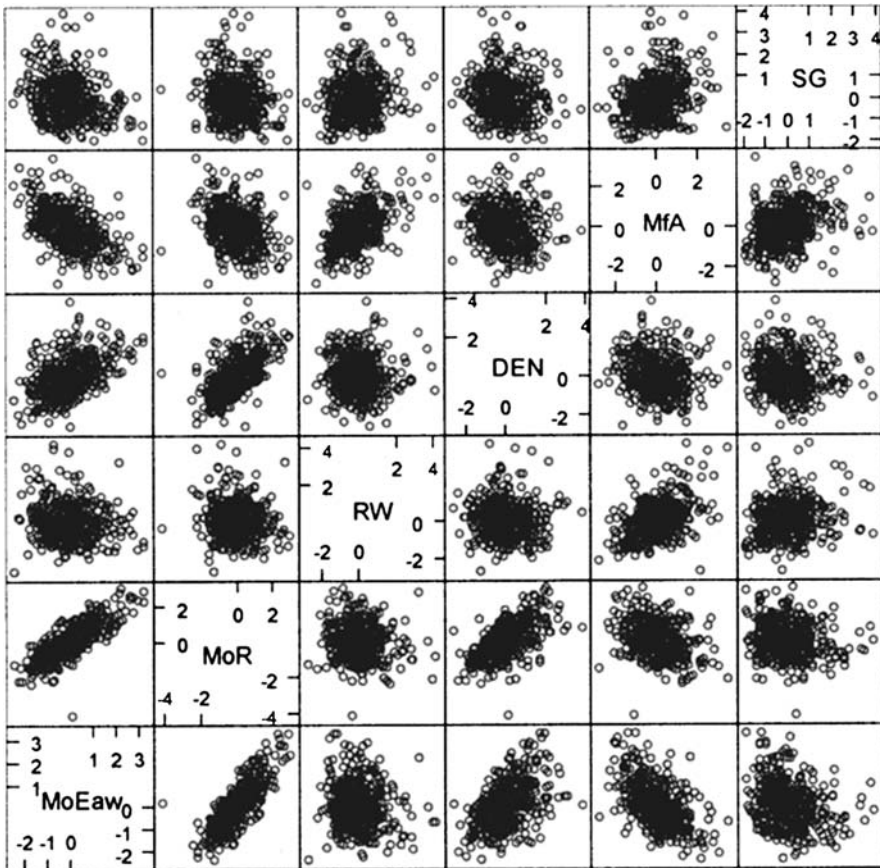
Fig. 2 Relationships between six wood variables used in path analyses
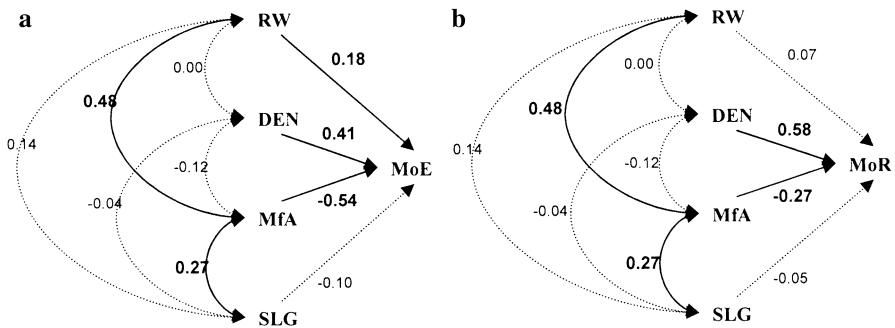
Fig. 3 Path analyses for Flynn site. **a** MOE$_{bil}$ (multiple $R^2 = 0.49$) and **b** MOR$_{bil}$ (multiple $R^2 = 0.45$) with direct effects indicated as *straight arrows* and indirect paths indicated as *curved lines* with correlation coefficients

Lower DEN and higher MFA are likely to be the cause of low strength in juvenile corewood of radiata pine. DEN in our study showed a stronger direct effect on wood strength than MFA. For example, the direct effect of DEN on MOR was consistently higher than the effect of MFA at all sample strata (e.g. Flynn billets pc$_{DEN\_MoR}$ = 0.58 vs. pc$_{MFA\_MoR}$ = −0.27). The stronger relationship of MOR with DEN than with MFA was also indirectly confirmed by comparing the relationship between MOR and SWV, which was also consistently less related to MOR than DEN (e.g. pc$_{VEL\_MOE}$ = 0.21 pc$_{DEN\_MOE}$ = 0.40).

Our path analyses confirmed a previous finding by Downes et al. (2002) that the predicted MOE$_{ss}$ from SilviScan is very strongly determined by MFAss (pc$_{MFA,MOE}$ = −0.87). However, when average billet values were used to estimate MOE, MFA had a somewhat smaller direct effect on MOE$_{bil}$ than on predicted MOE$_{ss}$ from SilviScan (pc$_{MFA\_MOE}$ = −0.64).

The direct effect of SLG on either MOE or MOR was insignificant. However, SLG and MFA may act jointly because of a significant positive correlation between them (Table 3; Fig. 3). Higher SLG angle also reduces the strength because wood is much stronger along the grain than across the grain. This holds in general for "cross grain" in structural lumber and boards, and corewood stiffness seems to be less sensitive to SLG than outerwood stiffness (Tsehaye and Walker 1996). Since MOE here was a measurement on a short clear sample it is affected mostly by microfibrils. However, they are not always aligned directly longitudinally with the sample axis. The microfibrils will be at some average angle, a function of MFA and SLG as well as other lesser factors such as relative contributions of the various secondary wall layers. In some samples MFA and SLG could combine to either enlarge or cancel each other out to some extent.

Prediction of stiffness and strength using component traits

Indirect prediction of stiffness using component traits has been shown to be possible (Evans and Ilic 2001). DEN and MFA have a major influence on mechanical performance of clear samples, and the two traits combined can predict MOE and

MOR reliably (Donaldson 1996; Cown et al. 1999). In our study, the combination of RW_{ss}, DEN_{ss}, and MFA_{ss} showed good prediction for MOE_{bil} at Flynn ($R^2 = 0.506$) and Kromelite ($R^2 = 0.490$). Adding SLG to RW_{ss}, DEN_{ss}, and MOE_{ss} measurements did not significantly improve the regression (result not presented).

Paddle-pop dynamic MOE_{pp} had the better prediction of billet MOE_{bil} at Flynn ($R^2 = 0.71$, Table 4) than SilviScan. However, MOE_{pp} had a lower prediction level at Kromelite ($R^2 = 0.310$). Adding increment core DEN_{ic} to MOE_{pp} did not increase R^2 significantly.

Both the IML[®] hammer measurement of stiffnes (MOE_{iml}) and that measurement plus full increment core density DEN_{ic} showed almost as good fit ($R^2 = 0.47$ and $R^2 = 0.48$ for Flynn, respectively and $R^2 = 0.40$ and $R^2 = 0.40$ for Kromelite, respectively) as the combined data from SilviScan increment core measurements. Inclusion of other growth and quality traits such as DBH and stem straightness, branch size, and branch angle scores only slightly increased the R^2 values. Table 4 also indicates that, whether using increment core measurements, IML or paddle-pop readings, predicted R^2 is always higher for outer-rings than for inner-ring samples.

Table 4 Prediction goodness of fit statistics R^2 for stiffness of billet, outer-rings and inner-rings clear samples (MOE_{bil}, MOE_{out}, and MOE_{in}) and strength of billet, outer-rings and inner-rings samples (MOR_{bil}, MOR_{out}, and MOR_{in})

	RW_{ss} and DEN_{ss}	RW_{ss}, DEN_{ss}, and MOE_{ss}	MOE_{iml}	MOE_{iml} and DEN_{ic}	MOE_{iml} DBH, STEM, BRS, BRA, and DEN_{ic}	MOE_{pp}	MOE_{pp} and DEN_{ic}
MOE_{bil}							
F	0.15	0.51	0.47	0.48	0.49	0.71	0.71
K	0.06	0.49	0.40	0.40	0.42	0.31	0.30
MOE_{out}							
F	0.15	0.51	0.52	0.53	0.54	0.71	0.72
K	0.09	0.54	0.43	0.44	0.45	0.29	0.32
MOE_{in}							
F	0.14	0.26	0.20	0.22	0.32	0.39	0.41
K	0.08	0.31	0.16	0.19	0.20	0.14	0.22
MOR_{bil}							
F	0.13	0.22	0.13	0.18	0.18	0.61	0.62
K	0.07	0.19	0.13	0.15	0.16	0.03	0.16
MOR_{out}							
F	0.13	0.24	0.18	0.23	0.24	0.65	0.65
K	0.09	0.22	0.16	0.19	0.20	0.16	0.17
MOR_{in}							
F	0.06	0.11	0.04	0.10	0.14	0.40	0.41
K	0.04	0.09	0.02	0.05	0.07	0.08	0.09

Predictive models include: (1) SilviScan RW_{ss} and DEN_{ss}; (2) SilviScan RW_{ss}, DEN_{ss}, and MOE_{ss}; 3) IML[®] hammer MOE_{iml}; (4) MOE_{iml} and increment core DEN_{ic}; (5) MOE_{iml}, DBH, STEM (Stem straightness), BRS (Branch size), BRA (Branch angle) and DEN_{ic}; (6) Paddle-pop dynamic MOE_{pp}; and (7) MOE_{pp} and DEN_{ic} for Flynn (F) and Kromelite (K)

Since SilviScan measurement MOE_{ss} costs more than measurement of MOE_{pp}, MOE_{iml}, and density (gravimetric method), use of MOE_{pp} or MOE_{iml} and gravimetric density for prediction of billet MOE_{bil} might be preferred methods. However, one concern is that paddle-pop samples were more adjacent to samples used for calculating billet MOE_{bil}. This proximity may render the paddle-pop measurements an advantage relative to SilviScan and IML measurements. Both paddle-pop and IML sample only the outer portion of the wood and any explanatory power of inner wood properties would be solely by co-variation.

For wood strength (MOR) multiple regression prediction was less precise (Table 4). Paddle-pop dynamic MOE_{pp} had the best prediction to billet MOR_{bil} at Flynn ($R^2 = 0.61$). The increment core measurements using SilviScan or IML hammer measurement had regression of $R^2 = 0.22$ and $R^2 = 0.18$, respectively, for Flynn site. Based on these weak regression relationships for strength, only Paddle-pop MOE_{pp} or IML measurement MOE_{iml} plus DEN_{ic} (gravimetric method) might be useful to predict billet strength.

Wood shrinkage

Pith-to-bark variation and correlation between shrinkage and other wood traits

Pith-to-bark variability of TS, RS, and LS was very high. There was an increase in transverse shrinkage, and a rapid decrease in LS from pith-to-bark. Averages for RS, TS, and the ratio TS/RS, LS, basic density (DEN), dynamic MOE, of the shrinkage samples (B, C, and D, Fig. 1) are listed for the whole billet, inner-rings, and outer-rings in Table 5.

Correlations between inner-rings and outer-rings (0.183 for RS, 0.167 for TS and 0.321 for LS) were low but significant at $P = 0.01$ level.

Due to relatively large errors in measuring RS and TS of the rings next to the pith, the relationships between transverse shrinkage and other wood traits were examined only for outer rings (3–6). RS and TS had a weak linear relationship with

Table 5 Sample means for inner-rings (rings 1–2) and outer-rings (rings 3–6) and weighted averages for whole billet at Flynn (F) and Kromelite (K) site

Trait	RS (%)	TS (%)	TS/RS	LS (%)	DEN_{sc}[a] (kg/m^3)	MOE_{sc} (GPa)
Billet						
F	3.44	5.64	1.67	0.59	375	5.33
K	3.10	5.25	1.75	0.71	333	4.90
Inner-rings						
F	2.86	4.35	1.58	1.31	329	3.33
K	2.58	3.98	1.61	1.37	299	2.86
Outer-rings						
F	3.64	6.10	1.71	0.33	392	6.17
K	3.29	5.76	1.99	0.47	346	5.64

[a] DEN_{sc} and MOE_{sc} based on three small clear samples (BCD)

DEN ($r^2 = 0.15$ and $r^2 = 0.13$, respectively) and MOE ($r^2 = 0.16$, $r^2 = 0.14$, respectively). However, LS in inner rings (1–2) had a strong negative non-linear relationship with MOE ($r^2 > 0.58$) and acoustic velocity ($r^2 > 0.78$) (Fig. 4).

Correlations among shrinkage and wood quality traits of the outer rings (rings 3–6) are listed in Table 6. RS and TS were positively correlated, but they were both negatively correlated with LS ($r < -0.41$). Correlation between LS and SLG was not significant. RS and TS were positively correlated with DEN while LS was strongly negatively correlated with MOE ($r < -0.66$), and positively correlated with MFA ($r > 0.42$). Correlations generally similar in magnitude were obtained for LS with the other traits using the inner samples (rings 1–2).

Causation from path analyses

A hypothesis has been proposed for explaining the anisotropic transverse shrinkage, based on the result that radial cell walls in pine latewood are about 25% thicker and have greater lignification than tangential walls. Furthermore, there is a tendency of preferential orientation of the fibrils in both cell walls in the general tangential direction (Gu et al. 2001). Slope of grain transfers a portion of TS in the longitudinal direction, and at individual fibre level MFA, would also act in a similar fashion (Panshin and de Zeeuw 1980). In juvenile wood of fast grown trees with wide rings, ring curvature has a similar effect as SLG.
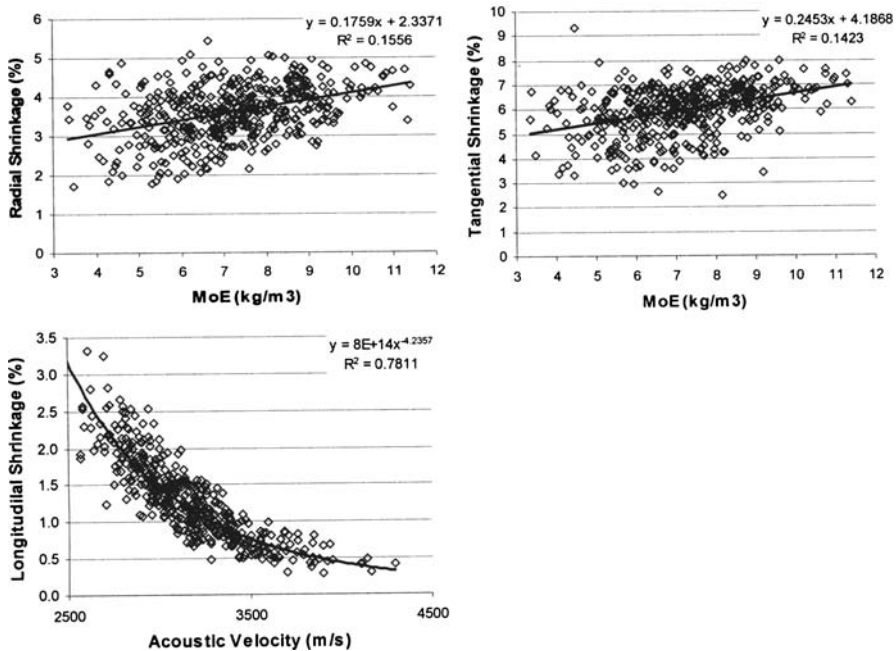

Fig. 4 Relationship between RS, TS and LS, and MOE for the measurements taken on block samples (**B**, **C**, and **D**). The upper panels are for TS and RS of outer wood samples (rings 3–6) at Flynn, and the *lower panel* represents data for the inner (rings 1–2) samples at Flynn

Table 6 Correlations for outer-rings (upper-diagonal for Flynn and lower-diagonal for Kromelite. Correlations in bold are $P < 0.01$)

RS	**0.54**	**-0.64**	**-0.42**	-0.06	**0.46**	**0.36**	**-0.17**	-0.03	Flynn
0.38	**TS**	**0.27**	**-0.53**	**-0.17**	**0.25**	**0.37**	**-0.17**	-0.01	
-0.69	**0.32**	T/R[a]	0.01	-0.09	**-0.28**	-0.08	0.03	0.04	
-0.44	**-0.41**	**0.15**	LS[b]	0.14	-0.08	**-0.66**	**0.42**	0.15	
0.08	-0.09	**-0.14**	**-0.22**	**RW**	0.03	**-0.16**	**0.41**	0.035	
0.35	0.12	**-0.216**	-0.02	-0.03	**DEN**	**0.39**	-0.09	-0.02	
0.37	**0.33**	-0.11	**-0.77**	0.12	**0.27**	**MOE**	**-0.63**	**-0.21**	
-0.05	-0.15	-0.06	**0.42**	**0.25**	0.03	**-0.62**	**MFA**	**0.21**	Kromelite
-0.08	-0.09	0.01	**0.19**	0.04	-0.06	**-0.24**	**0.132**	**SLG**	

[a] Square-root arc-sine transformed data

[b] Log transformed data

Path diagrams for variables RS, TS, LS, and RW, DEN, MFA, and SLG for outer rings at Flynn are presented in Fig. 5a–c. Density influenced transverse shrinkage more, but MFA had a stronger effect on LS. For example, path analyses revealed that
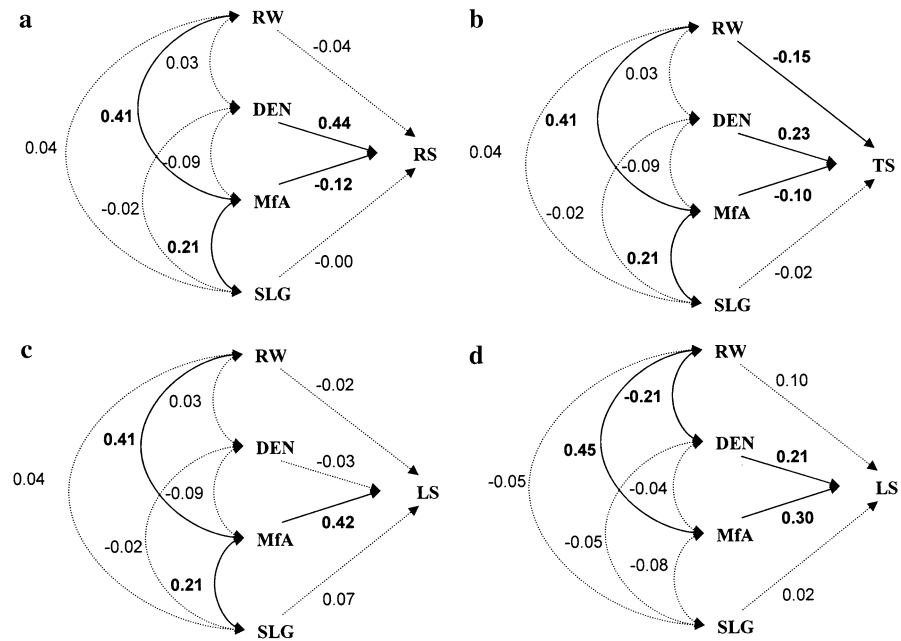
Fig. 5 Path analyses diagrams for Flynn samples: **a** radial shrinkage, **b** tangential shrinkage, **c** longitudinal shrinkage for outer-rings, and **d** longitudinal shrinkage for inner-rings

Table 7 Prediction goodness of fit statistics R^2 for RS_{out}, TS_{out}, and LS_{out} of outer-rings and LS of inner-rings

	Site	RW_{ss} DEN_{ss}	RW_{ss}, DEN_{ss} MFA_{ss}	MOE_{iml}	MOE_{iml} DEN_{ic}	MOE_{pp}
RS_{out}	F	0.16	0.18	0.06	**0.18**	0.10
	K	0.16	**0.17**	0.01	0.12	0.03
TS_{out}	F	0.08	0.09	0.06	**0.09**	0.08
	K	0.05	**0.09**	0.04	0.07	0.03
LS_{out}[a]	F	0.02	0.20	0.21	**0.22**	**0.26**
	K	0.06	**0.32**	0.18	0.21	0.16
LS_{in}[a]	F	0.04	0.13	0.07	**0.13**	0.08
	K	0.04	**0.24**	0.06	0.07	0.11

Predictive models include: (1) increment core RW_{ss} and DEN_{ss}, (2) increment core RW_{ss}, DEN_{ss}, and MFA_{ss}, (3) IML[®] hammer MOE_{iml}, and (4) MOE_{iml} plus DEN_{ic} for Flynn (F) and Kromelite (K). Models with R^2 significant are bold

[a] Log-transformed data

RS was influenced mainly by DEN ($pc_{DEN,RS} = 0.44$, $P < 0.001$) and to a lesser extent by MFA ($pc_{MFA\_RS} = -0.12$, $P = 0.012$), with multiple $R^2 = 0.224$. RW had a small indirect effect through MFA (Fig. 5a). Similarly, TS was influenced mainly by DEN ($pc_{DEN\_TS} = 0.23$, $P < 0.001$) and to a lesser extent by RW ($pc_{RW\_TS} = -0.11$, $P = 0.002$) and MFA ($pc_{RW\_TS} = -0.10$, $P = 0.043$) with multiple $R^2 = 0.099$. RW had small indirect effect through MFA (Fig. 5b).

In contrast, LS at Flynn (outer rings), was significantly influenced only by MFA ($pc_{MFA\_LS} = 0.42$, $P < 0.001$). However, at Kromelite there was evidence of influence by RW ($P < 0.001$), MFA ($P < 0.001$) and SLG ($P < 0.005$). Multiple $R^2 = 0.31$. Again RW might also have some small indirect effect through MFA (Fig. 5c). For inner rings at Flynn LS was significantly influenced by MFA ($pc_{MFA\_LS} = 0.30$, $P < 0.001$) and DEN ($pc_{DEN\_LS} = 0.21$, $P < 0.001$) (Fig. 5d). At Kromelite, besides MFA and DEN, there was also evidence of influence by RW ($P < 0.005$, $R^2 = 0.30$). Although R^2 values were generally low with about 20% of variation explained by RS and TS, and around 30% explained by LS, the F values and model significance were generally high ($P < 0.001$).

Prediction of RS, TS, and LS using component wood traits

The IML hammer measurement MOE_{iml} plus core gravimetric density (DEN_{ic}) were significant predictors of shrinkage traits at the Flynn site (Table 7). Increment core measurements using SilviScan RW_{ss}, DEN_{ss}, and MFA_{ss} were significant predictors of shrinkage at the Kromelite site. However, predictions only accounted for less than 30% of variation except for LS_{out} at Kromelite.

Conclusion

- Variation between inner- and outer-rings was larger than that among trees for stiffness and strength, and MOE and MOR were lower (50%)

in inner-rings (rings 1–2 from pith) than for outer-rings (rings 3–6 from pith);

- DEN had a higher correlation with MOR than with MOE, while MFA had a higher correlation with MOE than with MOR. SLG had higher correlation with MOE than with MOR;
- Path analyses revealed that the direct effect of DEN on MOR was greater than that of MFA, while the direct effect of MFA on MOE was greater than that of DEN;
- For wood stiffness, small axial ('paddle-pop') samples were the best for predicting billet MOE_{bil} at Flynn ($r^2 = 0.71$), however, that may be due to their vicinity to the benchmark samples (Fig. 1). SilviScan measurements provided good prediction for MOE for both sites ($R^2 > 0.49$). However, IML hammer measurements showed similarly good fit as SilviScan measurements ($R^2 > 0.40$). Therefore, the acoustic velocity measurements seem to be the most practical method for predicting billet stiffness in young trees;
- For wood strength, 'paddle-pop' samples showed the best prediction for billet MOR_{bil} at Flynn ($r^2 = 0.61$), but again, that may be due to their vicinity to the benchmark samples. SilviScan measurements provided low prediction power for MOR for both sites ($R^2 < 0.24$). IML hammer measurements plus core density showed similar fit as SilviScan measurements ($R^2 < 0.18$). Acoustic velocity and increment core density measurements seem to be the most practical method for predicting billet strength in young trees;
- Variation in shrinkage between inner- and outer-rings was larger than that among trees and RS and TS were higher (30–50%) for outer-rings than inner-rings, but LS decreased rapidly (>200%) from inner-rings to outer-rings. The ratio of TS:RS:LS was about 20:10:1 in outer-rings;
- RS and TS had a weak, significant linear relationship with DEN and MOE while LS had a strong negative non-linear relationship with MOE;
- In path analysis direct effect of DEN on RS and TS was greater than that of MFA, but MFA had a strong direct effect on LS;
- For wood shrinkage, multiple regression predictions were weak ($R^2 < 0.22$), but acoustic velocity combined with increment core density were the most practical measurements.

Generally, based on current results for juvenile wood stiffness, strength, and shrinkage multiple regressions using IML hammer combined with increment core density would be the most practical measurements. Results of this study and other studies (Kumar 2004; Dungey et al. 2006; Kumar et al. 2006; Matheson et al. 2008) indicate that for large scale (e.g. breeding purposes) evaluation of stiffness, indirect (acoustic) measurements may be more effective than measurements of component traits such as density or MFA. Breeding to improve juvenile corewood properties requires large numbers of standing trees (progenies) to be evaluated non-destructively so that superior individuals can be selected as parents (Dungey et al. 2006). Acoustic tools for measuring wood stiffness in logs and boards have been developed in the last few years (Walker and Nakada 1999). Tools for measuring SWV in standing trees such as IML Hammer, Director ST300, and

Fakopp are also commercially available (Carter et al. 2006; FibreGen 2006). The different acoustic tools give similar estimates of velocity and MOE in standing trees (Kumar et al. 2002; Matheson et al. 2008).

Based on our results, the use of acoustic tools such as IML hammer together with increment core density for prediction of wood stiffness, strength, and stability in evaluations of young genetic trials is recommended. The velocity of sound wave propagation has been shown to be a good predictor of radiata pine wood stiffness and LS. Phenotypic correlations between velocity and static MOE both measured in small axial beams are typically very high (Harding et al. 2002; Ilic 2004; Wu et al. 2005). However, using axial beams, MOE is measured over only a very short distance of clearwood (about 150–300 mm), while standing tree MOE_{iml} sometimes encompasses branch whorls up the stem and so a perfect correlation with the stress wave velocity would not be expected. Although small axial beams provide a rapid method for assessing both stiffness and strength as well as shrinkage of outer wood, they are not completely non-destructive and cost effective in terms of the time required for sampling. On the other hand, given that very young trees (with only six rings) were examined, the full power that SilviScan data can provide (i.e. radial variation profile) was not fully utilised in these evaluations.

References

AS/NZS 1748 (1997) Timber-stress-graded—product requirements for mechanically stress-graded timber. Joint Australian/New Zealand Standard

AS/NZS 4063 (1992) Timber-stress-graded-in-grade strength and stiffness evaluation. Joint Australian/New Zealand Standard

Astley J, Harrington J, Tang S, Booker R (1997) Finite element modelling of wood performance. FRI bulletin no. 202, pp 39–41

Barber NF, Meylan BA (1964) The anisotropic shrinkage of wood: a theoretical model. Holzforschung 18:146–156

Booker RE, Sorensson CT (1999) New tools and techniques to determine mechanical wood properties. FIEA, wood quality symposium, emerging technologies for evaluating wood quality for wood processing, Melbourne, December 1999

Burdon RD, Kibblewhite RP, Walker JCF, Megraw RA, Evans R, Cown DJ (2004) Juvenile versus mature wood: a new concept, orthogonal to corewood versus outerwood, with special reference to *Pinus radiata* and *P. taeda*. For Sci 50(4):399–415

Carter P, Chauhan S, Walker J (2006) Sorting logs and lumber for stiffness using Director HM200. Wood Fiber Sci 38(1):49–54

Cave ID (1969) The longitudinal modulus of *Pinus radiata*. Wood Sci Technol 3:40–48

Cave ID (1972) A theory of the shrinkage of wood. Wood Sci Technol 6:284–292

Cave ID, Walker JCF (1994) Stiffness of wood in fast-grown plantation softwoods: the influence of microfibril angle. Forest Prod J 44(5):43–48

Cown DJ (1999) New Zealand pine and Douglas-fir: suitability for processing. Forest research bulletin no. 216, p 72

Cown D, van Wyk L (2004) Profitable wood processing—what does it require? Good wood! NZ J For 49(1):10–15

Cown DJ, McConchie DL, Young GD (1991) Radiata pine: wood properties survey. FRI-bulletin no. 50

Cown DJ, Haslett AN, Kimberley MO, McConchie M (1996a) The influence of wood quality on lumber drying distortion. Annales Sci For 53:1177–1188

Cown DJ, Walford B, Kimberley MO (1996b) Cross-grain effect on tensile strength and bending stiffness of *Pinus radiata* structural lumber. NZ J For Sci 25(2):256–262

Cown DJ, Hebert J, Ball R (1999) Modelling radiata pine lumber characteristics. Part 1: mechanical properties of small clears. NZ J For Sci 29(2):203–213

Donaldson LA (1996) Effect of physiological age and site on microfibril angle in *Pinus radiata*. IAWA J 17(4):421–429

Downes GM, Hudson IL, Raymond CA, Dean GH, Michell AJ, Schimleck LR, Evans R, Muneri A (1997) Sampling plantation eucalypts for wood and fibre properties. CSIRO Publishing, Collingwood, VIC, Australia, p 132

Downes GM, Nyakuengama JG, Evans R, Northway R, Blakemore P, Dickson RL, Lausberg M (2002) Relationship between wood density, microfibril angle and stiffness in thinned and fertilized *Pinus radiata*. IAWA J 23(3):253–265

Dumail JF, Castera P (1997) Transverse shrinkage in maritime pine juvenile wood. Wood Sci Technol 31:251–264

Dungey HS, Matheson AC, Kain D, Evans R (2006) Genetics of wood stiffness and its component traits in *Pinus radiata*. Can J For Res 36(5):1165–1178

Evans R (2003) Wood stiffness by X-ray diffractometry. In: Proceedings of the workshop, characterisation of the cellulosic cell wall, Grand, Lake, Colorado, 25–27 August 2003. University of Iowa and the Society of Wood Science and Technology, Madison

Evans R, Ilic J (2001) Rapid prediction of wood stiffness from microfibril angle and density. For Prod J 51:53–57

Evans R, Stuart SA, Van der Tour J (1996) Microfibril angle scanning of increment cores by X-ray diffractometry. Appita J 49(6):411–414

FibreGen (2006) Director ST300. Accessible from: http://www.fibrgen.com/products.html [accessed 01 November 2006]

Gapare WJ, Wu HX, Abarquez A (2006) Genetic control of the time of transition from juvenile to mature wood in *Pinus radiata* D. Don. Ann For Sci 63:871–878

Gapare WJ, Hathorn A, Kain D, Matheson AC, Wu HX (2007) Inheritance of spiral grain in the juvenile core of *Pinus radiata* D. Don. Can J For Res 37:116–127

Gapare WJ, Ivković M, Powell MB, McRae TA, Wu HX (2008) Genetics of shrinkage in juvenile trees of radiata pine from two test sites in Australia. Silvae Genet 57(3):145–151

Gu H, Zink-Sharp A, Sell J (2001) Hypothesis on the role of cell wall structure in differential transverse shrinkage of wood. Holz Roh-Werkst 59:436–442

Hansen JK, Roulund H (1998) Spiral grain in a clonal trial with Sitka spruce. Can J For Res 28:911–919

Harding KJ, Greaves BM, Gorsser C, Copley TR (2002) Juvenile wood quality in *Pinus* plantations: selecting clones with superior stiffness for structural timber. In: Nepveau G (ed) Fourth workshop: "connection between forest resources and wood quality: modelling approaches and simulation software". Harrison Hot Springs, Canada, pp 94–103

Harris JM (1997) Shrinkage and density of radiata pine compression wood in relation to its anatomy and formation mode. NZ J For Sci 7:91–106

Harris JM, Meylan BA (1965) The influence of microfibril angle on longitudinal and tangential shrinkage in *Pinus radiata*. Holzforschung 19:144–153

Haslett AN, Simpson IG, Kimberley MO (1992) Utilisation of 25-year-old *Pinus radiata*. Part 2: warp of structural timber in drying. NZ J For Sci 21(2/3):228–234

Ilic J (2001a) Relationship among the dynamic and static elastic properties of air-dry *Eucalyptus delegatensis* R. Baker. Holz Roh-Werkst 59:169–175

Ilic J (2001b) Paddle-pop sticks—not just for licking. 27th forest products research conference, CSIRO forestry and forest products, Melbourne, Session 5, pp 45–46

Ilic J (2003) Dynamic MOE of 55 species using small wood beams. Holz Roh-Werkst 61(3):167–172

Ilic J (2004) Effect of juvenile core on softwood processing: results from recent resource and wood quality studies. In: Wood quality 2004—practical tools and new technologies to improve segregation of logs and lumber for processing. Albury, 5–6 August 2004

Johansson M (2003) Prediction of bow and crook in timber studs based on variation in longitudinal shrinkage. Wood Fiber Sci 35(3):445–455

Johansson M, Bäkström M (2002) Distortion models based on variation in material poperties. BC meeting. In: Nepveau G (ed) Fourth workshop: "connection between forest resources and wood quality: modelling approaches and simulation software". Harrison Hot Springs, BC, pp 337–345

Kingston RST and Risdon CJE (1961) Shrinkage and density of Australian and other south–west Pacific wood. CSIRO division of forest products. Technical paper No. 13

Kumar S (2004) Genetic parameter estimates for wood stiffness, strength, internal checking and resin bleeding for radiata pine. Can J For Res 34:2601–2610

Kumar S, Jayawickrama KJS, Lee J, Lausberg M (2002) Direct and indirect measures of stiffness and strength show high heritability in a wind-pollinated radiata pine progeny test in New Zealand. Silvae Genet 51:256–261

Kumar S, Dungey HS, Matheson AC (2006) Genetic parameters and strategies for genetic improvement of stiffness in radiata pine. Silvae Genet 55(2):77–84

Li CC (1981) Path analysis—a primer. The Boxwood Press, Pacific Groove

Mack JJ (1979) Australian methods for mechanically testing small clear specimens of timber. CSIRO, division of building research technological paper (second series) No. 31

Matheson AC, Yang JL, Spencer DJ (1997) Breeding radiata pine for improvement of sawn timber value. In: Zhang SY, Gosselin R, Chauret G (eds) Timber management toward wood quality and end-product value. Proceedings of CTIA/IUFRO international wood quality workshop. IV–19, Quebec

Matheson AC, Gapare WJ, Ilic J, Wu HX (2008) Inheritance and genetic gain in wood stiffness in radiata pine measured acoustically in young standing trees. Silvae Genetica 57(2):56–64

McKinley R, Ball R, Downes G, Fife D, Gritton D, Ilic J, Koehler A, Morrow A, Pongracic S (2003) Resource evaluation for future profit: wood property survey of the green triangle region. http://www.fwprdc.org.au/menu.asp?id=36&lstReports=16 [accessed 01 November 2006]

Megraw RA, Leaf G, Bremer D (1998) Longitudinal shrinkage and microfibril angle in loblolly pine. In: Butterfield BG (ed) Proceedings of IAWA/IUFRO workshop on "microfibril angle in wood". University of Canterbury, New Zealand, pp 27–61

Megraw R, Bremer D, Leaf G, Roers J (1999) Stiffness in loblolly pine as a function of ring position and height and its relationship to microfibril angle and specific gravity. In: Nepveu G (Ed) Proceedings of the third workshop IUFRO S5.01.04 "Connection between silviculture and wood quality through modeling approaches and simulation software", La Londe-Les Maures, France, 5–12 September, pp 341–349

Meylan BA (1967) Cause of high longitudinal shrinkage in wood. For Prod J 18:75–78

Pang S (2002) Predicting anisotropic shrinkage of softwood Part 1: theories. Wood Sci Technol 36:75–91

Panshin AJ, de Zeeuw C (1980) Textbook of wood technology, 4th edn. p 772

SAS Institute Inc (2005) SAS System 8.02. Online reference manual. SAS Institute Inc., Cary

Tsehaye A, Walker JCF (1996) Spiral grain in Canterbury *Pinus radiata*: within- and between-tree variations and effect on mechanical properties. New Zealand J For Sci 25(3):358–366

Walker JCF, Nakada R (1999) Understanding corewood in some conifers: a selective review on stiffness and acoustics. Int For Rev 1:251–259

Wu HX, Ivković M, McRae TA, Powell MB (2005) Breeding radiata pine to maximise profit from solid wood production: summary report PN01.1904. Forest and wood products research and development corporation, Melbourne. http://www.fwprdc.org.au/menu.asp?id=36&lstReports=16

Xu P, Walker JCF (2004) Stiffness gradients in radiata pine trees. Wood Sci Technol 38(1):1–9

Xu P, Donaldson L, Walker J, Evans R, Downes G (2004) Effects of density and microfibril orientation on the vertical variation of low-stiffness wood in radiata pine butt logs. Holzforschung 58(6):673–677

Ying L, Kretschmann DE, Bendtsen BA (1994) Longitudinal shrinkage in fast-grown loblolly pine plantation wood. For Prod J 44(1):58–62

Zobel BJ, Sprague JR (1998) Juvenile wood in forest trees. Springer, Berlin, p 300